Energy Conversion and Management 300 (2024) 117931

Contents lists available at ScienceDirect

Energy Conversion and Management

journal homepage: www.elsevier.com/locate/enconman

Decarbonisation pathways of the cement production process via hydrogen and oxy-combustion

Franco Williams [a,*], Aidong Yang [a], Daya Ram Nhuchhen [b,c]

[a] Department of Engineering Science, University of Oxford, Parks Road, Oxford OX1 3PJ, United Kingdom
[b] Energy Division, Government of Northwest Territories, Yellowknife, NT, Canada
[c] Canadian Energy Systems Analysis Research Initiative, University of Calgary, Calgary, AB, Canada

ARTICLE INFO

Keywords:
Cement production
Deep decarbonisation
Hydrogen fuel
Indirect calcination
Oxy-combustion
Energetic assessment

ABSTRACT

Decarbonising cement production is of profound importance for meeting global greenhouse gas emission reduction targets and mitigating the impact of climate change. This study evaluates various technical options for achieving deep decarbonisation in a clinker production facility by utilising hydrogen (H_2) as an alternative fuel to replace fossil fuels and by integrating an oxy-combustion technique with carbon capture and storage (CCS). Using Aspen Plus process simulations, we examined the extent of decarbonisation and assessed the thermal and electrical energy demands. This was achieved by incorporating an amine-absorption-based CO_2 capture to a conventional natural gas fuelled reference plant, implementing oxyfuel-combustion of natural gas, and exploring four different scenarios for replacing fossil fuel with H_2. In these scenarios, H_2 was assumed to be produced through on-site water electrolysis, which also supplied oxygen for oxyfuel combustion, potentially eliminating the need for an air separation unit (ASU). The processes utilizing H_2, except for the case of indirectly heated pre-calcination, employed oxyfuel combustion. The results indicate that the natural gas-fuelled oxyfuel-combustion process had the lowest total energy input at 4.92 GJ/t clinker, approximately 35% lower than that of the reference plant. Processes using H_2 reduced energy demand by 11% in the H2-d scenario and 33% in the H2-a scenario. However, the process with indirect calcination required 6.24 GJ/t clinker, about 8% more H_2 fuel than direct calcination but helped eliminate the need for an ASU. The results also reveal that greater H_2 substitutions led to higher total process energy requirements due to the inefficiencies of the electrolysis process. While the H_2-using processes could reduce the CO_2 generation by up to 559 kgCO_2/t clinker, this represents only about 27.6% of the CO_2 reductions relative to the reference plant. These findings underscore the limitation of fuel substitution alone in cement production and emphasize the need for innovations in raw materials and the adoption of CCS to achieve deeper decarbonisation in cement industries.

1. Introduction

Tackling climate change requires the rapid reduction of greenhouse gas (GHG) emissions from all sectors of the global economy. The construction sector faces significant challenges, as it is projected to consume 35–60 % of the remaining carbon budgets for the 2 °C scenario over the decades leading to 2050. This projection is driven by anticipated population growth and socioeconomic progress [1]. Cement production, responsible for about 8 % of global carbon dioxide (CO_2) emissions [2], has widely been identified as a primary target for progressive decarbonisation efforts.

In the conventional cement production process, CO_2 emissions primarily result from the production of clinker, the main component of Portland cement [3]. Specifically, two main sources of CO_2 emissions exist: (1) process emissions from the calcination process, where limestone ($CaCO_3$), a key component in the raw meal for clinker production, decomposes into lime (CaO) and CO_2, and (2) energy emissions from the combustion of fossil fuels (mainly coal or natural gas) to provide the required thermal energy for both the calciner and the kiln, where calcining and sintering reactions occur. Extensive research has explored ways to reduce CO_2 emissions from calcination by replacing clinker with supplementary cementitious materials [4], like fly ash [5], and ground granulated blast furnace slag (GGBS) [6], which do not involve limestone decomposition [7].

* Corresponding author.
E-mail addresses: franco.williams@eng.ox.ac.uk (F. Williams), aidong.yang@eng.ox.ac.uk (A. Yang), daya.nhuchhen@ucalgary.ca (D.R. Nhuchhen).

https://doi.org/10.1016/j.enconman.2023.117931
Received 9 August 2023; Received in revised form 14 October 2023; Accepted 23 November 2023
Available online 30 November 2023

Regarding energy consumption, the cement industry's substantial demand, averaging approximately 4GJ per tonne of cement [8], contributes to 12–15 % of total global industrial energy consumption [9], primarily from fossil fuels. Various strategies have been proposed to reduce GHG emissions and energy consumption [10], including improvements in fuel efficiency [11], such as heat recovery from flue gases using the Organic Rankine Cycle (ORC) [12], and the use of alternative fuels such as biomass [4], and hydrogen (H_2) [13]. As alternative fuels have different physical and chemical properties, the selection of alternative fuels that have minimal impacts on combustion phenomena and the overall cement production process is critical [14].

To address unavoidable emissions from calcination or fuel combustion, carbon capture and storage (CCS) becomes essential [15]. Oxyfuel combustion [16], where combustion is with pure oxygen instead of air [17], has been considered a favourable approach for CCS, preventing the mixing of nitrogen with CO_2 from calcination or fuel combustion [18].

In line with other industrial sectors emphasizing the decarbonisation of thermal energy supply [2], the use of H_2 as a zero-carbon fuel in cement production has gained significant interest from both academia [19], and industry [20]. A modelling study by the Mineral Products Association [19], evaluated the reduction in coal consumption in the kiln by replacing thermal energy demand with 20 % H_2, 70 % biomass, and 10 % plasma energy, resulting in the elimination of 100 % fossil CO_2 emissions. Another study [13] achieved a 44 % reduction in CO_2 emissions for the total system by entirely replacing coal-based fuel with H_2 in the kiln. Furthermore, research conducted by [2] utilised H_2 from alkaline electrolysis to obtain natural-gas-enriched hydrogen (10 % H_2 in volume) in the kiln, replacing 50 % of coal by weight and estimating a 15 % to 20 % reduction in CO_2 emissions compared to pure coal-based cement production. In industry, Hanson conducted trials at a cement plant using a mixture of 20 % H_2 in volume mixed with biomass and plasma energy at Ribblesdale Cement Works, aiming to supply net zero carbon concrete by 2050. The results indicated that if this mixture were applied in the kiln, approximately 180,000 tonnes of CO_2 could be saved annually [21].

Despite these emerging explorations, research on the use of H_2 in cement production is currently limited, and there is a lack of systematic comparisons of possible H_2-based technical schemes and other decarbonisation options. In this work, we present technical modelling of six process options, distinguished by fuel, combustion oxygen supply, and CO_2 capture arrangement, for clinker production. We assess and compare their energy consumption and CO_2 production. To our knowledge, this is the first study to compare process options with different levels of H_2 substitution for natural gas in oxyfuel combustion (which facilitates CO_2 separation and capture) with the conventional process equipped with amine-based (post-combustion) carbon capture and oxyfuel combustion. Previous studies have considered the use of oxygen as a by-product of water electrolysis [17], as a potentially advantageous alternative to an energy-intensive air separation unit (ASU) for supplying oxygen to cement production [15]. In our study, on-site water electrolysis was assumed to supply both H_2 and O_2 for feeding the oxyfuel combustors. To reduce the demand for oxygen, one of the novel process options includes indirect calcination, where combustion for heat supply occurs separately from the decomposition of limestone. This separation keeps combustion products separate from the CO_2 produced by calcination, ensuring high CO_2 purity in the captured CO_2 stream. While previous research has explored indirect calcination in connection with fossil fuels [22], our study investigates its application with H_2. Overall, the results of this work provide a consistent comparison of the energy consumption and CO_2 production among the selected process options, serving as a foundation for future techno-economic assessments.

2. Methods

In this section, we first provide a brief overview of the technical options for clinker production assessed in this work (Section 2.1), followed by a detailed description of the modelling of these options as implemented in Aspen Plus (Section 2.2). Subsequently, the approach to modelling CO_2 separation and compression associated with the clinker production processes (Section 2.3) and quantifying energy consumption (Section 2.4) are presented, along with the key assumptions adopted in modelling and analysis (Section 2.5).

2.1. Overview of technical options

This work involves the technical modelling of six process options for clinker production, which were differentiated based on fuel use, combustion oxygen (O_2) supply, and CO_2 capture arrangements. Table 1 provides an overview of the characteristics of these compared processes. Concerning the extent of H_2 substitution, it is worth noting that there are significant differences in combustion characteristics between H_2 and conventional fuels, which has raised caution about extensive H_2 usage in clinker production [13], particularly in the kiln [2]. However, there is limited experimental evidence available to determine the feasible range. Among the process options involving H_2, three processes (H2-a, H2-b, and H2-c) reduced the natural gas usage in the kiln to a conservative 80 % (by vol.) of the oxyfuel process, with the remaining thermal energy met by the supplementary H_2. In contrast, H2-d represents a hypothetical scenario exploring the potential outcome of complete H_2 substitution. In terms of the calciner, the process H2-a did not incorporate H_2 substitution, while the other three H_2 processes assumed the use of 100 % H_2, a configuration that had previously been examined through theoretical modelling of calcination as a standalone process (i.e., not as part of clinker production) [19].

2.2. Modelling of clinker production processes

The mathematical modelling in this study was based on literature data, primarily sourced from a plant in Alberta, Canada, that produces 4,200 tonnes of clinker in a day [17]. As shown in Fig. 1, the process involves preheating the raw meal to 800 °C (in the pre-heater) using the calciner exhaust gas before it enters the calciner, where limestone decomposition occurs at 900 °C, achieving 95 % calcination [23]. The solid output from the calciner then enters the kiln, where further decomposition, transition and sintering reactions take place [15], reaching a sintering temperature of 1500 °C [17]. While the resulting clinker from the kiln is cooled to approximately 100 °C by cooling air (in the cooler), the exhaust gas from the kiln is fed into the calciner. Both the cooling air and the preheater exhaust gas undergo heat recovery processes by the Organic Rankine Cycle (ORC). The specific configuration of this heat recovery system varies depending on the chosen process and must provide a hot gas flow of 1,762 kg/tonne clinker at 176.85 °C to operate the vertical roller mill (VRM) [34].

All six process options (Figs. 1-6) were simulated (refer to Supplementary Figs. S1–S6) for the detailed Aspen models) with an input of 1.6 tonnes/hr of raw meal and a clinker output of 1 tonne/hr. It is important to note that all produced CO_2 was captured in its pure form at 150 bar with 100 % capture efficiency, preparing it for subsequent transport and storage (not modelled in this study).

For the Aspen simulation, the base physical property method "SOLIDS" was selected, and solid-containing streams were represented in the stream class "MIXCISLD", which included two sub-streams of "MIXED" and "CISOLID".

2.2.1. Reference (NG) process for clinker production

In the reference process (NG) depicted in Fig. 1, and with its Aspen flowsheet presented in Supplementary Fig. S1, natural gas combustion in the presence of air was used to supply thermal energy for clinker production (NG-C and NG-K in Supplementary Fig. S1). Both combustors, for the calciner and the kiln, were modelled as a stoichiometric reactor (RStoic), (CALCINER and COMB-K in Supplementary Fig. S1).

Table 1
Aspen processes parameters.

Process Options	Combustion		Oxygen supply	Calcination Mode	CO_2 capture
	Calciner	Kiln			
NG (reference case)	100 % Natural gas	100 % Natural gas	N/A	Direct	Amine-based capture + compression
Oxy	O_2 + 100 % Natural gas	O_2 + 100 % Natural gas + 0 % H_2	ASU	Direct	Compression, cooling, and separation (with refrigeration for water separation)
H2-a	O_2 + 100 % Natural gas	O_2 + 80 % Natural gas + 20 % H_2	ASU + electrolysis	Direct	
H2-b	Air + 100 % H_2	O_2 + 80 % Natural gas + 20 % H_2	Electrolysis	Indirect	
H2-c	O_2 + 100 % H_2	O_2 + 80 % Natural gas + 20 % H_2	ASU + electrolysis	Direct	
H2-d	O_2 + 100 % H_2	O_2 + 100 % H_2	Electrolysis	Direct	

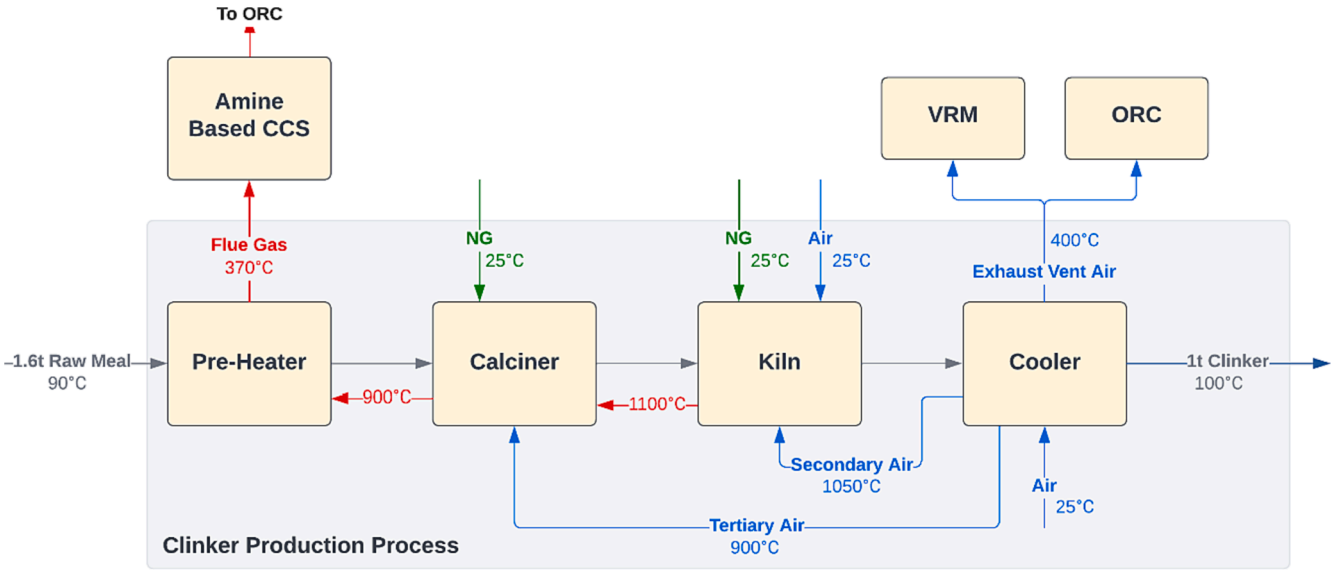

Fig. 1. NG cement production process flow diagram (natural-gas reference case), adopting amine-based carbon capture, (See Supplementary Fig. 1 for Aspen Flowsheet).

Series of solid reactions occurring in the kiln were simulated using three RStoic reactors, representing decomposition, transition (i.e., exothermic reaction zone), and sintering stages (DECOMP, TRANSI, and SINTER in Supplementary Fig. S1). Details of the modelled reactions at each stage are provided in Table 2, with conversion rates set to ensure that the resulting clinker maintains the expected chemical compositions, including tricalcium silicate (C_3S), dicalcium silicate (C_2S), tricalcium aluminate (C_3A), and tetra-calcium aluminoferrite (C_4AF), within the specified range [17]. That is, these conversions were calculated based on the assumed raw meal composition and the anticipated composition of the calcined meal and clinker. Specifically, the resulting mass fractions of these components in the clinker were 0.691, 0.111, 0.072, and 0.126, respectively.

In the NG process as per Fig. 1, primary and secondary air were introduced into the combustor of the kiln (COMB-K), while tertiary air was supplied to the combustor of the calciner (COMB-C). Secondary and tertiary air were pre-heated to temperatures of 1050 °C and 900 °C, respectively [17], by recovering heat from the hot clinker. The exhaust vent air (output of the cooler in Fig. 1) was effectively utilised to recycle energy back into the system for operating the vertical raw mill (VRM). In the NG process with the CCS implementation, the exhaust vent air was initially used to provide heat to the CCS operation. Afterwards, the airflow was separated, with one portion dedicated to meeting the VRM requirements (VRM-IN) and the other excess flow was used to operate the organic Rankine cycle (ORC) (ORC-IN) for heat recovery. Additionally, the pre-heater flue gas was harnessed to operate the ORC for heat recovery.

Heat losses were considered in the model, consistent with [15], for both the calciner and different stages of the kiln. The heat loss values are as follows; 42.99 MJ/t clinker for the calciner, 30.60 MJ/t clinker for the decomposition stage, 59.40 MJ/t clinker for the transition stage, and 90 MJ/t clinker for the sintering stage, respectively. These same heat loss values were assumed for all subsequent process options.

The reference model developed and simulated here in the Aspen Plus process simulation software was based on the Excel-based model presented by Nhuchhen et al. [17], for a natural gas-fired cement plant. However, this study incorporated three key modifications: i) the kiln stage was modelled with three distinct stages (decomposition, transition, and sintering), taking into account heat losses. In contrast, the previous model in [17], treated the kiln as a single stage; ii) the O_2 concentrations in the flue gases for the kiln and calciner exits were adjusted to 6.5 % and 1.0 % (molar basis), respectively, in the reference paper [17], whereas in this study, the supply of O_2 was set to achieve more complete consumption, resulting in O_2 concentrations at 3.7 % and 0.3 % (molar basis) for these two streams, respectively; iii) this work did not consider the leakage air, a factor taken into account in [17].

2.2.2. *Modified process for clinker production using oxy-combustion*

To model the process referred to as Oxy (as shown in Fig. 2; and detailed in Supplementary Fig S2. for the Aspen flowsheet), the Aspen

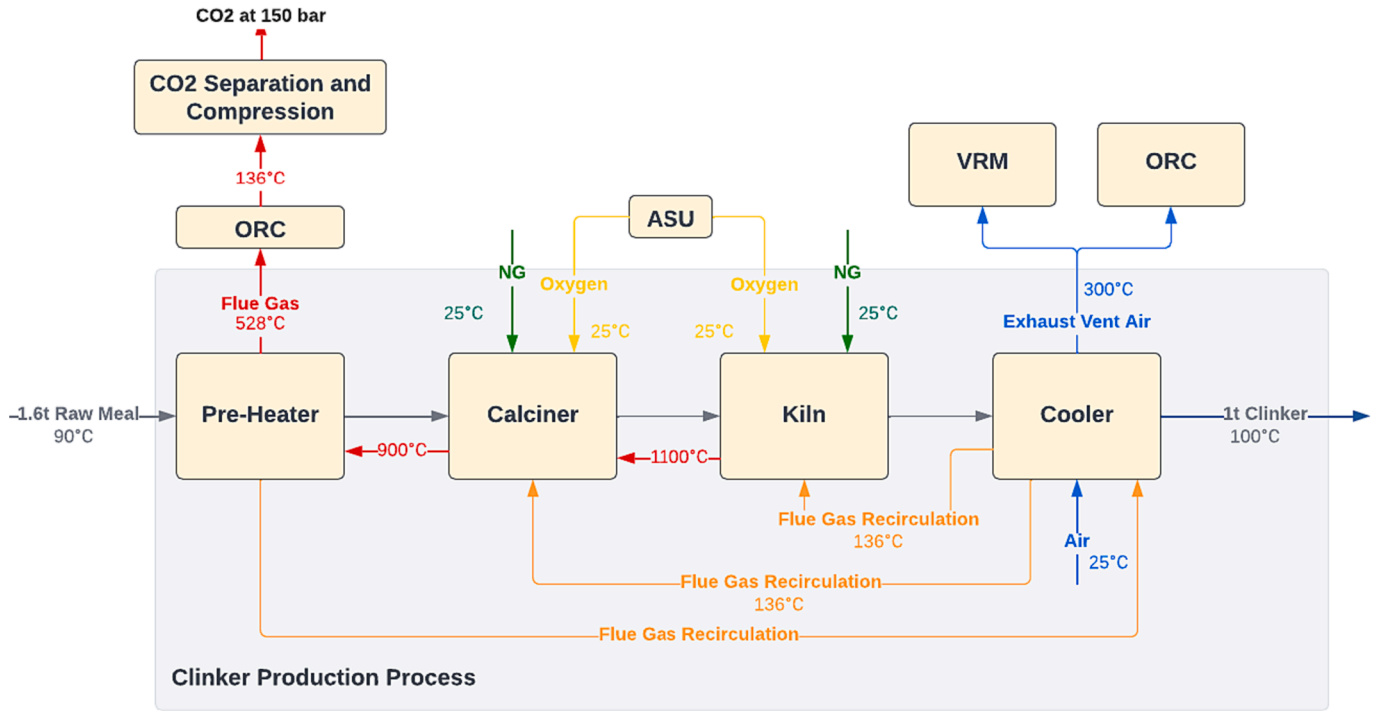

Fig. 2. Oxy cement production processes flow diagram (oxyfuel-combustion based), with CO_2 separation and compression, (See Supplementary Fig. 2 for Aspen Flowsheet).

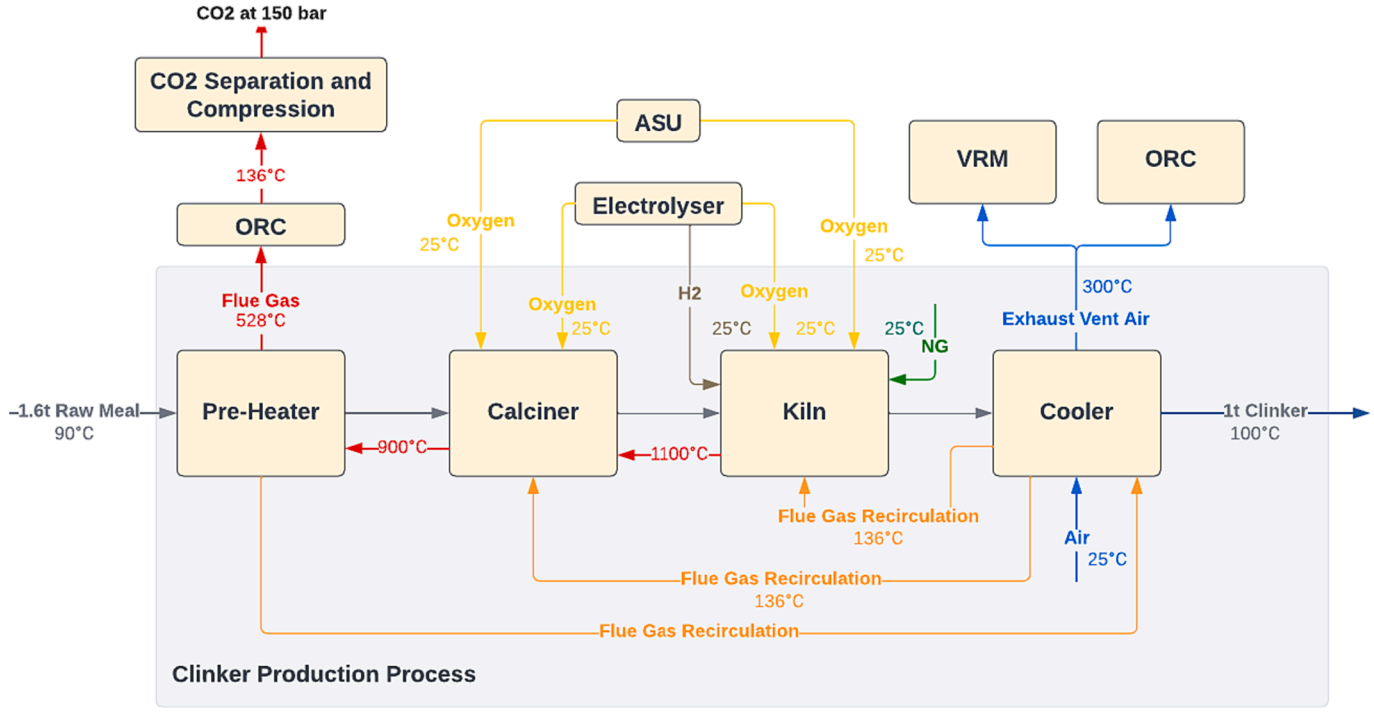

Fig. 3. H2-a cement production process flow diagram (20% hydrogen replacement of natural-gas in the kiln coupled with oxygen combustion), with CO_2 separation and compression, (See Supplementary Fig. 3 for Aspen Flowsheet).

model used for the process NG was adapted. This adaptation involved replacing the air input to the kiln and calciner combustors with O_2 at 25 °C as per Fig. 2, for natural gas combustion (O2-IN-KILN and O2-IN-CALCINER in Supplementary Fig. S1). Flue gas recirculation (FGR) at 136 °C was employed to maintain adequate gas flows throughout the system, following the approach outlined in [17]. More specifically, the flue gas exiting the preheater tower was divided into three separate streams. Two of these streams were designed to mimic the role of secondary air and tertiary air in the process NG, maintaining the same molar flow rates and target temperatures as in that process. The third flow became an exhaust stream.

All O_2 required for this process was assumed to be provided by a cryogenic distillation-based air separation unit (ASU) at an electrical energy demand of 0.81 GJ/tonne O_2 as indicated in [17] (though not

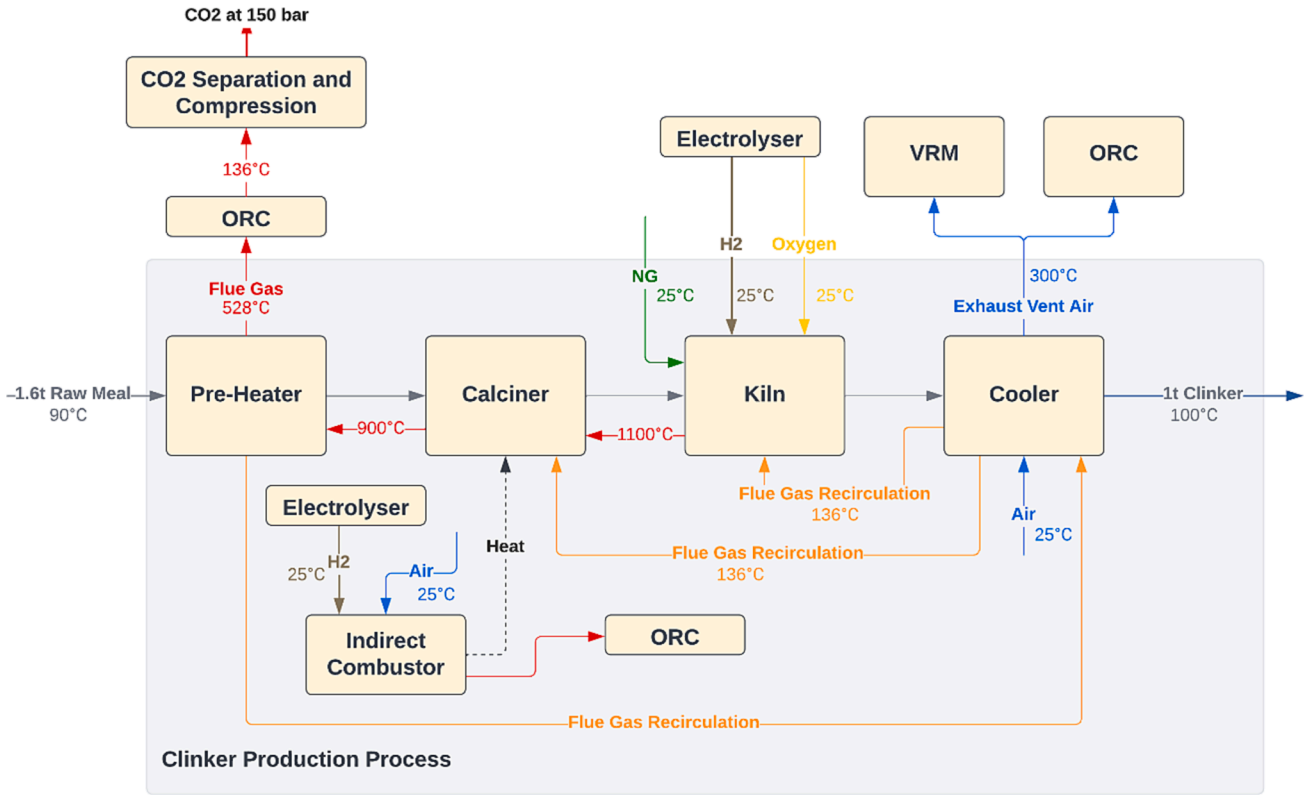

Fig. 4. H2-b cement production process flow diagram (indirect calcination using hydrogen for the calciner and direct combustion of hydrogen in the kiln), with CO_2 separation and compression, (See Supplementary Fig. 4 for Aspen Flowsheet).

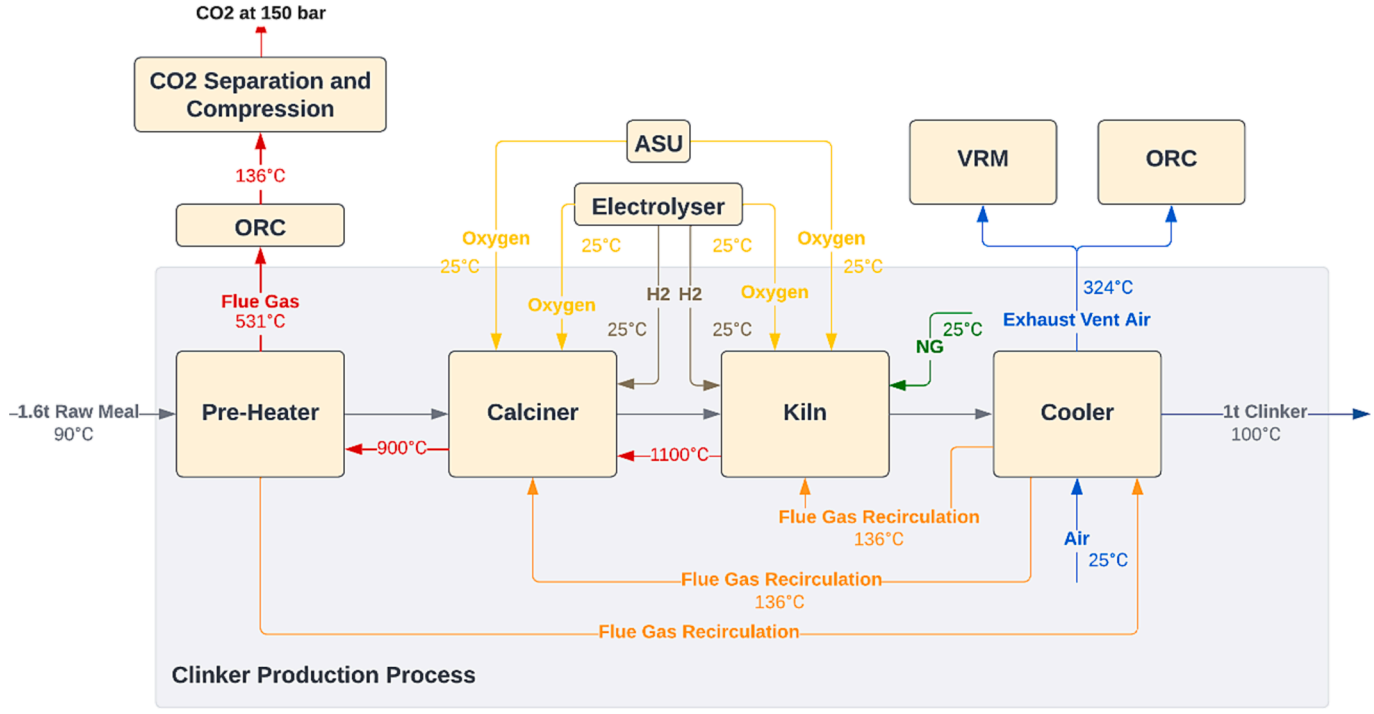

Fig. 5. H2-c cement production process flow diagram (20% natural-gas replaced with hydrogen in both the calciner and kiln), with CO_2 separation and compression, (See Supplementary Fig. 5 for Aspen Flowsheet).

explicitly modelled in this study). The natural gas feeds to the calciner and the kiln, along with the corresponding O_2 feeds, were adjusted to meet the temperature targets set for these units. The flow rates of exhaust vent air were more than sufficient to operate the VRM. Excess flows and the flows from the pre-heater flue gas were both incorporated into the system to operate the ORC for heat recovery. Pre-heating of the

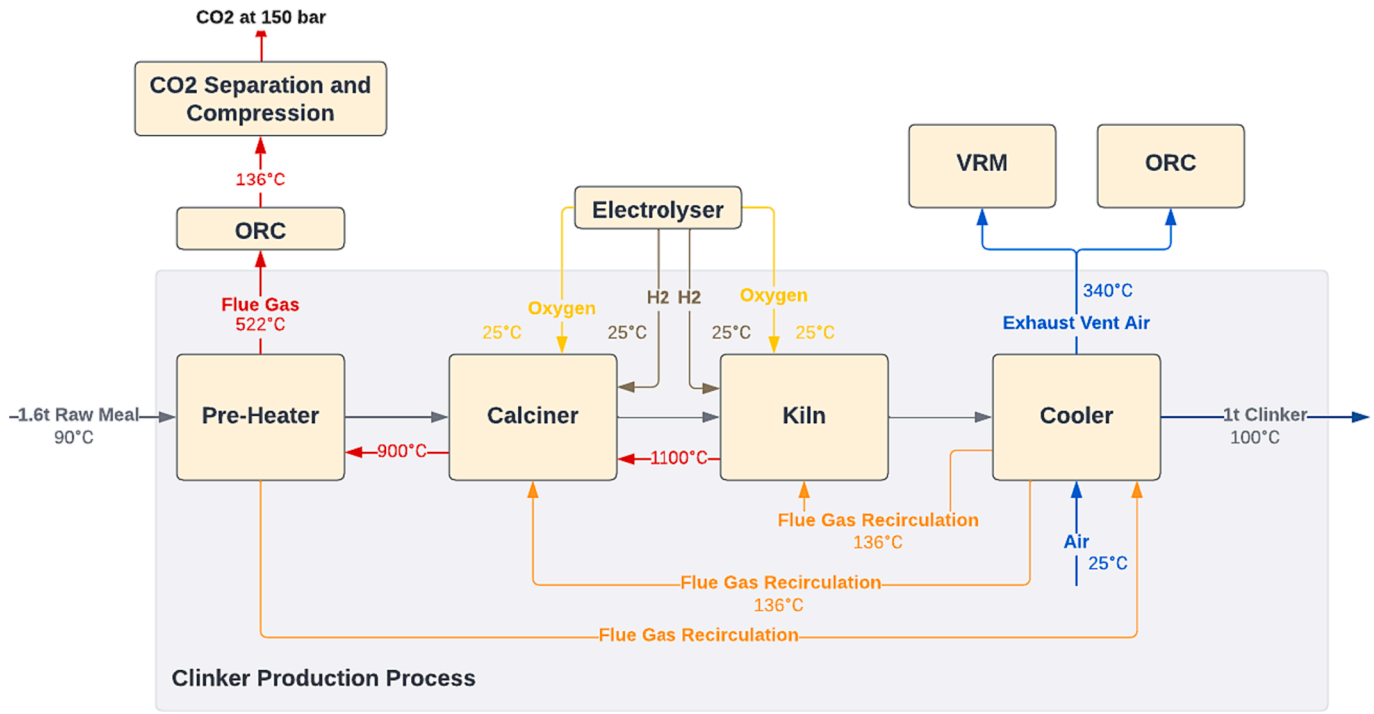

Fig. 6. H2-d cement production process flow diagram (100% hydrogen replacement of natural-gas and combustion with oxygen), with CO_2 separation and compression, (See Supplementary Fig. 6 for Aspen Flowsheet).

Table 2
Major reactions considered in the production process and the fractional conversions.

Reaction	Fractional Conversion of Component	Fractional Conversion
2 CaO(CISOLID) + SiO_2(CISOLID) –> C_2S(CISOLID)	SiO_2	1
C_2S(CISOLID) + CaO(CISOLID) –> C_3S(CISOLID)	C_2S	0.825
3 CaO(CISOLID) + Al_2O_3(CISOLID) –> C_3A(MIXED)	Al_2O_3	0.507
4 CaO(CISOLID) + Al_2O_3(CISOLID) + Fe_2O_3(CISOLID) –> C_4AF(CISOLID)	Fe_2O_3	1

O_2 input in both the calciner and kiln, achieved through heat recovery from the pre-heater flue gas, was set to 136 °C, in accordance with [17].

2.2.3. *Modified processes for clinker production using hydrogen*

The four processes involving the use of H_2 were modelled by adapting the model of Process Oxy (refer to Figs. 3 - 6, and Supplementary Figs S3 - S6). For processes H2-a, H2-c and H2-d, a direct replacement of natural gas by H_2 was implemented according to the degrees of substitution described earlier (as detailed in Table 1), without altering the process design. For process H2-b, indirect calcination was modelled by (1) feeding the calciner's combustor with air instead of O_2; (2) assuming a heat flow to the calciner from its combustor to the effect of bringing the temperature of the combustor's exhaust to 800 °C; and (3) injecting the tertiary air equivalent flow and the kiln exhaust into the calciner (as opposed to its combustor), to avoid the mixing of CO_2 in these two flows with N_2 brought in by the calciner's combustion air. As such, there are two separate exhaust gas flows arising from the calcination subsystem, one from the combustor (containing no CO_2) and another from the outlet of the calciner (as a mixture of CO_2 and water steam), therefore a modified heat recovery arrangement was adopted for process H2-b, as described below:

- The calciner's combustor (COMB-C in Supplementary Fig. S3) was supplied with air instead of O_2;
- A heat flow was assumed to be provided by the calciner's combustor to bring the temperature of the combustor's exhaust to 800 °C; and
- The tertiary air equivalent flow and the kiln exhaust were injected into the calciner (rather than its combustor) to prevent the mixing of CO_2 in these two flows with N_2 introduced by the calciner's combustion air. Consequently, two separate exhaust gas flows originate from the calcination subsystem: one from the combustor (containing no CO_2) and another from the outlet of the calciner (comprising a mixture of CO_2 and water steam). Therefore, a modified heat recovery arrangement was employed for process H2-b.

In all four processes, the supply of H_2 was assumed to be via on-site water electrolysis, which also produces O_2 to meet the demand for oxyfuel combustion either partially (H2-a, H2-c) or fully (H2-b, H2-d). The remaining O_2 demand in H2-a and H2-c was met by an ASU. The electricity consumption by electrolysis was considered at two efficiency levels based on the ratio of the lower heating value of produced H_2 and the electricity input: 60 % (reflecting the efficiency of contemporary industrial alkaline electrolysers [24]) and 84 % (achievable with more efficient technologies such as solid-oxide electrolysers [25]), corresponding to 50 and 40 kWh/kg H_2, respectively.

2.3. *CO_2 separation and compression*

In process NG, a standard amine-based system for CO_2 capture, which was not explicitly modelled, was assumed to have 100 % capture efficiency. This system was employed to produce a pure CO_2 stream at 1 bar, which was subsequently compressed to 150 bar as reported in [26], a pressure commonly chosen to facilitate the transportation of captured CO_2. The energy demand for CCS in process NG was calculated, and the results can be found in Table 5.

For all the other processes, the flue gas consisted of a mixture of CO_2 and water due to oxyfuel combustion. In these cases, CO_2 separation was integrated with compression, as illustrated in Fig. 7. The flue gas exiting

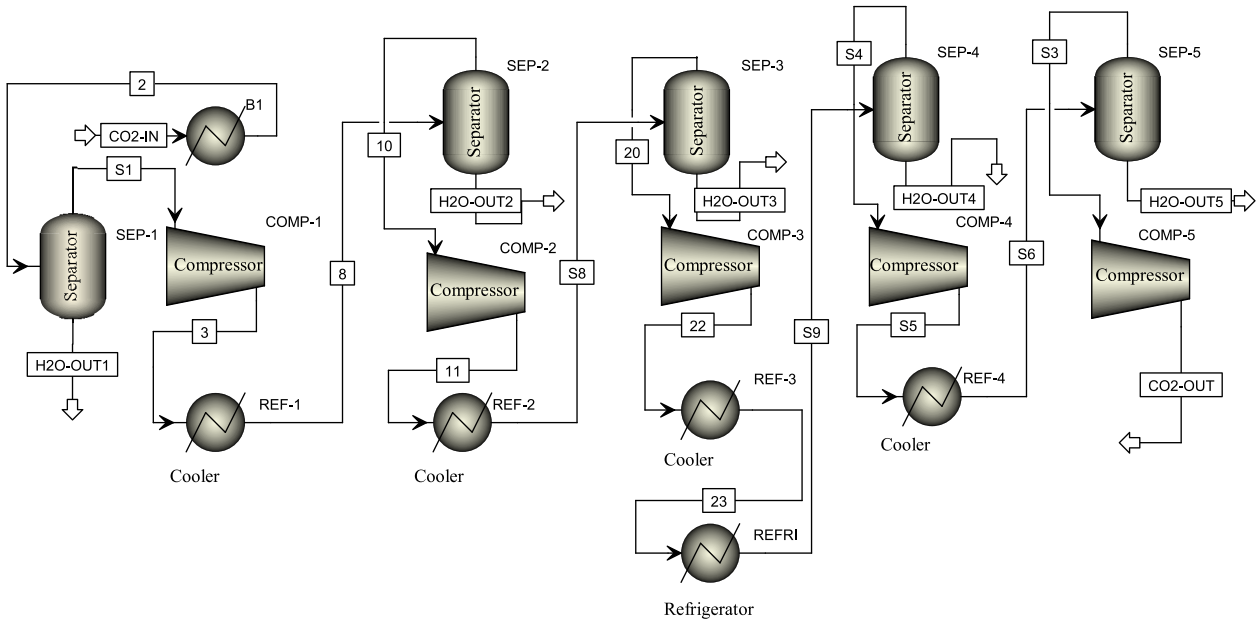

Fig. 7. CO_2 Separation and Compression model from Aspen simulations including four stages of separation, compression and cooling.

from each process underwent a cooling process, using cooling water as a refrigerant within the Aspen simulation. Liquid water resulting from the cooling process was removed in a liquid–vapor separator module. The flue gas then entered a four-stage compression process, with the same cooling and water separation steps repeated between stages while maintaining a temperature of 35 °C for the cooler output.

An exception was introduced after the third stage of water cooling (REF-3), where an additional refrigeration step (REFRI) was included to further reduce the temperature to 6 °C. This extra cooling facilitated additional water removal, ensuring that the final CO_2 product achieved a purity greater than 99.95 mol%. The output temperature leaving the final cooling stage (REF-4) was 35 °C. Following the fourth stage of water separation (SEP-4) and compression (COMP-4), the flow exited the process for transport and storage.

The simulation employed a pressure ratio of 2.72 and assumed isentropic and mechanical efficiencies of 0.85 and 0.95 respectively [27]. The electricity consumption (W) for the refrigeration cycle was estimated from the heat removed (Q) using a coefficient of performance (COP) value of 3.7 [28].

2.4. Energy recovery and consumption

The key components affecting the net energy consumption or production of the processes are summarized in Table 3. These components include natural gas fuel, fans, auxiliary equipment, CCS, and an ORC, which were present in all the process options. The energy consumption associated with the ASU and electrolysis was detailed in Section 2.2. Further explanations of the calculation of the other components are provided below.

Table 3
Key energy users and providers.

Energy users or providers	Processes	Energy Type	Contribution
Natural Gas Fuel	All	Thermal	Consumption
Fans	All	Electrical	Consumption
Auxiliary Equipment	All	Electrical	Consumption
Carbon Capture and Storage (CCS)	All	Electrical and Thermal	Consumption
Organic Rankine Cycle (ORC)	All	Electrical	Production
Air Separation Unit (ASU)	Oxy, H2-a, H2-c	Electrical	Consumption
Electrolysis	H2-a, H2-b, H2-c, and H2-d	Electrical	Consumption

The natural gas fuel input for each process was obtained from the Aspen simulation, and the thermal energy content was calculated using the lower heating value of methane, 50 MJ/kg [29].

The power consumption for each fan (W_{fan}), as described as below, was estimated by scaling the reported reference fan power consumption in [17]. Here, q_{ref} and W_{ref} represent the volumetric gas flow and the power consumption of a reference fan, while q is the volumetric gas flow of the fan.

$$W_{fan} = W_{ref} \times \left(\frac{q}{q_{ref}}\right)^3 \quad (1)$$

The auxiliary power consumption was assumed to remain constant across all processes as extracted from [17], at 245 MJ/t of clinker for auxiliary equipment.

The thermal energy required to operate amine-based carbon capture at 1 bar in process NG was primarily for operating the reboiler of the regeneration column at a temperature of 128.4 °C, requiring a heat input of $Q_{reb} = 3.8$ MJ/kg of CO_2 [30]. In the Aspen Plus simulation of process NG, the maximum coverage of heat demand through waste heat was achieved via heat recovery (Q_{rec}) from the flue gas and exhaust vent air by cooling the hot streams to 148.4 °C (allowing a 20 °C temperature difference for heat transfer with the reboiler). The net thermal energy demand ($Q_{net} = Q_{reb} - Q_{rec}$) for carbon capture was assumed to be supplied by natural gas combustion, and its CO_2 generation were included in the total CO_2 to be captured from the process NG (refer to Supplementary Fig. S1). Additional power consumption for carbon capture, (P_{add}) was assumed to be 0.55 MJ/kg of CO_2 [30]. The electricity consumption by the subsequent CO_2 compression in the process NG and that of CO_2 separation and compression in other processes were calculated based on the modelling described in Section 2.2.

An organic Rankine cycle (ORC) was integrated into the simulated processes for waste heat recovery to generate electricity in support of the processes. The ORC power ($W_{ORC} = Q_{in} \times Q_{in}$) was calculated using the recovered waste heat from the hot gas stream (Q_{in}). Q_{in} was obtained from the results of the Aspen simulation of each cooler, mimicking the evaporator of the ORC, on the waste heat source streams cooled to

130 °C, which was 20 °C higher (to provide a heat transfer driving force) than the working fluid's temperature within the ORC. It is typically around 110 °C, as presented in the ORC design from [31]. The efficiency (η_{th}) of the ORC was set to 0.225 according to the assumed organic working fluid [31].

2.5. Additional assumptions

Different assumptions and inputs applied for conducting the technical and energetic analysis are discussed below:

- The natural-gas molar composition consists of 100 % methane, with a lower heating value (LHV) of 50 MJ/kg.
- The molar composition of air was assumed to be 78.12 % N_2; 20.95 % O_2; and 0.93 % Ar.
- The clinker composition by weight percentage (13 % C_4AF, 11 % C_2S, 69 % C_3S, and 7 % C_3A) and raw meal input (refer to Supplementary Table S7) were kept constant across all processes.
- The pressure was assumed to be 1 bar throughout the clinker production system.
- Complete combustion was assumed for all combustors, with O_2 molar percentage less than 1 %.

3. Results and discussion

This section presents and discusses the modelling results in three interconnected parts. Firstly, we provide the key results of Aspen Plus simulation, focusing on materials flows and essential process parameters, particularly temperatures, in Section 3.1. Subsequently, we delve into an analysis of two critical aspects of process performance used for comparing the six technical options, namely energy consumption and CO_2 production, in Sections 3.2 and 3.3, respectively.

3.1. Simulated material flows and key process conditions

The key temperatures for calcination and sintering play a vital role in ensuring the intended chemical conversions occur in various stages of the system. As presented in Table 4, the simulated results show that they were tightly controlled for all processes around the target values of 900 °C and 1500 °C, respectively. These critical process temperatures were consequences of the fuel input in these processes. Furthermore, Table 4 indicates that the kiln exhaust temperatures, influenced by the control of the calcination and sintering temperatures, are slightly higher in the Oxy and H_2 processes compared to the reference process (NG). This difference is not expected to pose any significant operational issues. Detailed material flows in the major streams of all six processes examined here are provided in Supplementary Tables S1 - S6.

As shown in Table 5, the reference case (NG) consumes 77.54 kg/t clinker of natural gas (equivalent to 3877 MJ in fuel LHV) per tonne clinker, which falls within the anticipated range of fuel consumption by conventional cement plants [4]. In comparison, there is a modest increase of 4.9 % GJ in the natural gas fuel consumption in process Oxy. This increase is primarily due to changes in the composition of the combustion products and the gaseous flows within the system [17].

The fuel mix varies in cases involving H_2, as expected. Process H2-a exhibits modest H_2 substitution for natural gas, while processes H2-b and H2-c demonstrate greater substitution. Finally, process H2-d achieves complete substitution of H_2 for natural gas. Despite variations in the fuel input composition, the total fuel LHV remains similar, approximately 4067 MJ/t clinker, for processes Oxy, H2-a, H2-c, and H2-d. This represents a 4.8 % increase compared to the process NG (reference case). However, H2-b requires considerably higher fuel input, approximately 4310 MJ/t clinker, which is roughly ~ 11 % more than the reference case. This increase is mainly attributed to the use of air (rather than O_2) in the calciner combustor as part of the indirect calcination process. This results in a greater amount of flue gas, about 1471 kg/tonne clinker (~35 % more) compared to the process Oxy, leading to greater heat loss.

As expected, H2-b requires the least O_2 supply due to indirect calcination; eliminating the need for an ASU as electrolytic O_2 exceeds the demand. In the other processes, increased H_2 usage generally translates to reduced demand for O_2, determined by the combustion requirement. Process Oxy relies entirely on the ASU for O_2 supply. Conversely, process H2-d achieves an O_2 balance between the electrolysis energy generation and the consumption by 100 % H_2-based fuel combustion. Processes H2-a and H2-c fall between these extremes, relying on the ASU to varying degrees.

3.2. Energy consumption

As indicated in Table 5, the overall energy consumption encompasses both thermal energy input from fuels (natural gas and hydrogen) and electrical energy input for operating fans, auxiliary components of the cement plant, electrolysers, ASU, and CO_2 capture and separator units. This summary provides a comparative analysis of the energetic performance across different processes, considering both thermal and electrical energy demands, which are influenced by the energy efficiency of water electrolysis (η_{ely}). First, we analyse the results assuming $\eta_{ely} = 60$ %, and we present an energy flow diagram in Fig. 8 to illustrate the distribution of electrical (el) and thermal (th) energy across all the processes. It is worth noting that approximately 10 % to 13 % of the energy consumption is attributed to fans while 3 % to 6 % is attributed to CO_2 separation and compression, consistently across all processes. In the first three processes (NG, Oxy, and H2-a), the majority of the energy demand (>50 %) comes from natural gas in the form of thermal energy. In contrast, in processes H2-b, H2-c, and H2-d, electrolysis dominates the energy demand, primarily in the form of electrical energy.

In a previous study [2], it was found that half of the thermal energy demand was from natural-gas-infused H_2. In the H_2 processes (H2-a – H2-d), all the thermal energy demand is supplied by natural gas, as H_2 is sourced from electrolysis. Moreover, the thermal energy consumption in an oxy-combustion-based production process from the literature consumed around 560 MJ/tonne of clinker [15]; the thermal energy consumption in the simulated Oxy process was higher, at 4052 MJ/tonne of clinker; the difference could be attributed to result from the variation in adopted fuel type and modelling assumptions. More

Table 4
Key temperatures, flowrates, and thermal energy input from Aspen Plus modelling.

System Input	Key Temperatures (°C)		Natural Gas-In (kg/t clinker)		Oxygen-In (kg/t clinker)		Oxygen from ASU (kg/t clinker)	Hydrogen-In (kg/t clinker)		LHV of fuel input
	Calcination	*Sintering*	*Calciner*	*Kiln*	*Calciner*	*Kiln*		*Calciner*	*Kiln*	*MJ/t clinker*
NG	898.55	1500.03	47.00	30.54	N/A	N/A	0.00	N/A	N/A	3877.05
Oxy	899.24	1501.61	45.47	35.52	181.37	141.68	323.05	N/A	N/A	4049.08
H2-a	899.76	1498.75	45.60	28.41	181.91	136.69	295.34	N/A	2.91	4049.32
H2-b	899.68	1499.23	N/A	28.41	0.00	140.00	0.00	21.04	3.04	4310.34
H2-c	903.14	1498.24	N/A	28.41	165.00	132.00	119.35	19.47	2.736	4085.19
H2-d	899.01	1502.61	0.00	0.00	144.00	132.00	0.00	19.08	14.94	4082.40

Table 5
Component of thermal and electrical energy consumptions/production of all six process options for cement production decarbonisation.

Processes		NG	Oxy	H2-a	H2-b	H2-c	H2-d
Electrical Energy for production (MJ/t)	Fans	540.99	432.32	424.75	401.97	439.99	509.44
	Auxiliary	244.80	244.80	244.80	244.80	244.80	244.80
	Electrolysis (60 % Efficiency)	0.00	0.00	523.26	4334.76	3997.03	6123.60
	Electrolysis (84 % Efficiency)	0.00	0.00	418.61	3467.81	3197.63	4898.88
	ASU	0.00	261.67	239.23	0.00	96.68	0.00
	ORC	−105.02	−349.76	−349.71	−403.00	−360.68	−359.09
	Subtotal (60 % Electrolysis Efficiency)	680.77	580.03	1082.32	4578.53	4417.83	6318.75
	Subtotal (84 % Electrolysis Efficiency)	680.77	580.03	977.67	3711.58	3618.42	5294.03
Thermal Energy for production (MJ/t)	Natural Gas	3880.15	4052.32	3703.44	1421.64	1421.64	0.00
Energy for CO2 capture (MJ/t)	Amine-based capture: Electrical Energy	492.08	0.00	0.00	0.00	0.00	0.00
	Amine-based capture: CCS Thermal Energy	2233.93	0.00	0.00	0.00	0.00	0.00
	CO_2 Separation and Compression: Electrical energy	282.55	289.75	282.73	237.08	237.13	208.79
	Sub Total (MJ/t)	3008.56	289.75	282.73	237.08	237.13	208.79
Net Total Energy (MJ/t) with 60 % electrolysis efficiency		7569.48	4922.09	5068.50	6237.25	6076.59	6727.54
Net Total Energy (MJ/t) with 84 % electrolysis efficiency		7569.48	4922.09	4963.84	5370.29	5277.19	5502.82

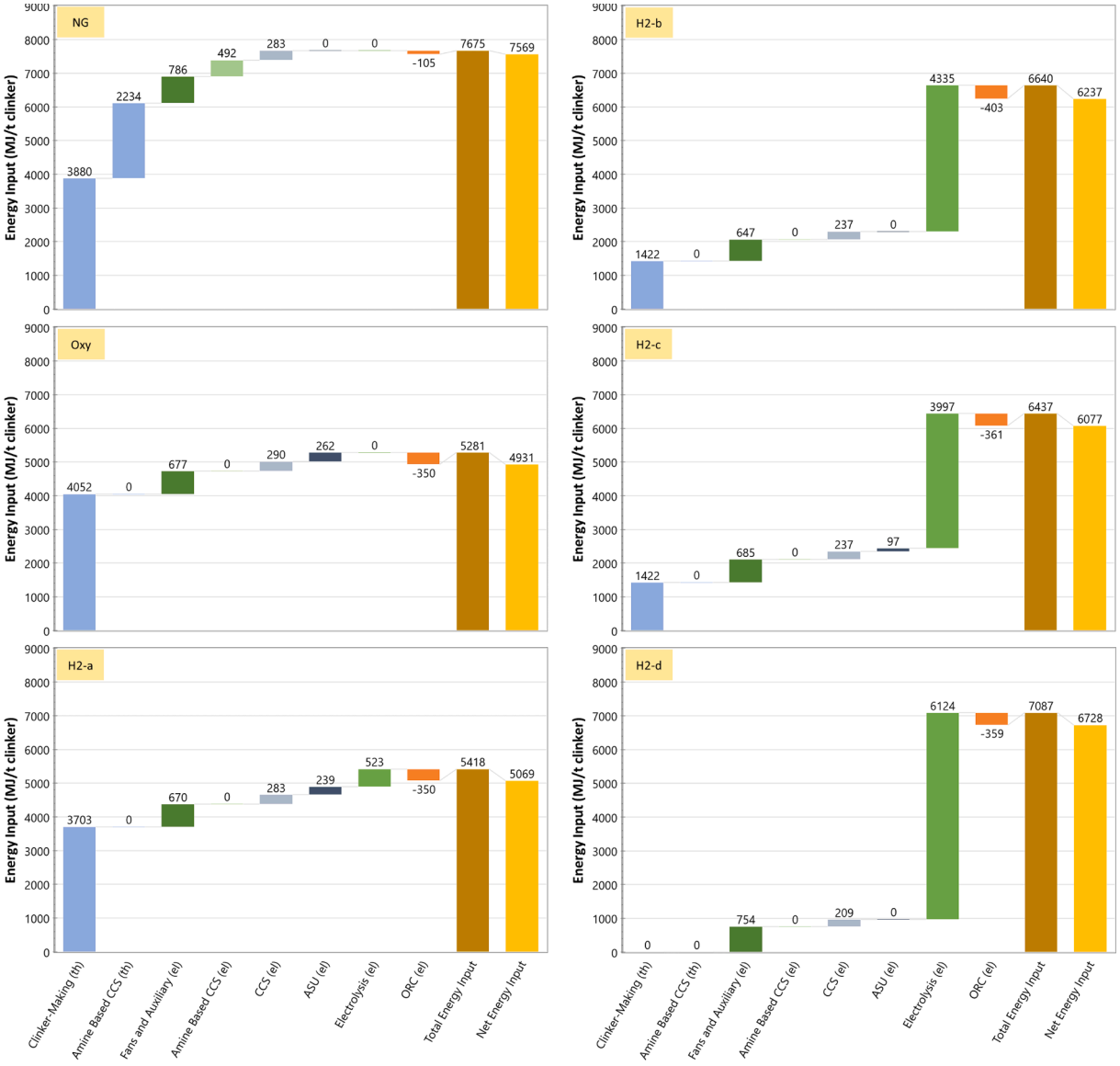

Fig. 8. Total and net energy flows in simulated processes (electrolysis efficiency = 60 %) [Note:Electricity sources were assumed to be 100% renewable (GJ_{el}=GJ_{th})].

importantly, according to [17], the thermal energy demand was 7 % higher compared to the NG-based process in the literature. This work confirmed the comparative trend between the two process options, although the difference is slightly lower, at 4.3 %.

The most energy-intensive is process NG, where CO_2 capture (including purification and compression) imposes a significant energy burden, accounting for approximately 40 % (3008.56 MJ/t clinker) of the total energy input. This is despite partial coverage of the thermal energy requirement for solvent regeneration by heat recovery from the clinker production process.

In contrast, process Oxy stands out as the most energy-efficient option. Although operating the ASU requires additional electrical energy, it constitutes only a small portion (~5% or 261.67 MJ/t clinker) of the total energy demand of the process Oxy. The use of oxyfuel combustion significantly simplifies CO_2 separation. Even with the ASU's energy requirement (261.67 MJ/t clinker) added to the energy consumption by CO_2 separation and compression (289.75 MJ/t clinker), the sum of the two energy demands is still much lower than the energy demand for the CO_2 capture of the process NG (3008.56 MJ/t clinker), resulting in substantial energy savings that offset the slight increase in its natural gas or thermal energy consumption during clinker production.

Across the hydrogen-involving processes (H2-a, H2-c, and H2-d), clear trends for electricity and natural gas demand emerge. As the level of H_2 substitution increases, electricity demand becomes significantly higher, driven by the requirement of electrolysis. Although natural gas demand decreases, the total fuel energy input in process H2-a is similar to that of the process Oxy (as shown in Table 5). The energy loss in electrolysis during the conversion from electricity to H_2 means that the greater the H_2 substitution, the greater the electrolytic energy demand for producing 1 tonne of clinker. Increased use of electrolytic H_2 results in i) more electrolytic O_2, reducing ASU operation and its energy demand, and ii) lower CO_2 production, reducing the energy demand for CO_2 separation and compression (also discussed in Section 3.3). However, these savings are not significant enough to offset the energy demand of electrolysis. As shown in Table 5, if $\eta_{ely} = 60$ %, the energy demand for the entire system in the H_2-using processes ranges from 5068.60 to 6727.54 MJ/t clinker, with electrolysis accounting for 10 % to 91 % of the net total energy consumption. On the other hand, these H_2-using processes reduce the energy demand by 11 % to 33 % compared to the reference process NG.

However, achieving a significantly higher electrolysis efficiency would be required for a process with significant H_2 substitution to energetically outperform process Oxy. The energetic performance of process H2-b is about 6 % less than H2-c (despite having the same level of H_2 substitution as H2-b). This difference is primarily due to the higher fuel input requirement caused by the use of air in the calciner combustor as part of indirect calcination. It managed to eliminate the need for an ASU while allowing the clinker to operate with 80 % of natural gas and oxyfuel combustion. However, the relative insignificance of the ASU in total energy consumption means that the increase in the higher fuel input requirement leads to an overall energy penalty. It is important to note that this process recovers approximately 15 % more electricity compared to the other oxyfuel processes, thanks to the higher waste heat content in the flue gas from the calciner combustor. However, the low efficiency of ORC (20 %) results in a considerable energy loss, highlighting the need for more energy-efficient energy recovery to improve the overall energetics of process H2-b.

3.3. CO_2 production and capture

The CO_2 produced for all the processes were calculated using the Aspen Plus simulations and are listed in Table 6. It is evident that the introduction of oxyfuel-combustion in the processes effectively eliminates nitrogen from the flue gases, with the exception of the calciner combustor exhaust from process H2-b. This exception occurred because air was introduced to burn H_2 in the indirect calcination combustor, as described earlier, resulting in only water vapour and nitrogen. The highest CO_2 molar fraction was 74 % in the flue gas from the H2-b process. Furthermore, increasing the replacement of natural gas with H_2 led to a reduction in the flue gas flow in processes H2-a, H2-c, and H2-d. This reduction in the flue gas flow subsequently reduces the need for CO_2 capture and separation, along with its associated electrical energy demand, from 283 MJ/t clinker in process H2-a to 209 MJ/t clinker in process H2-d (as indicated in Table 5).

As indicated in Table 6, even in the process H2-d where the fuel-related emissions were entirely eliminated by replacing natural gas with H_2, limestone calcination still contributed to about 559 $kgCO_2$/t clinker. It accounted for 72.4 % of the total CO_2 production, in the reference case (process NG). This highlights a limitation of fuel substitution as a decarbonisation strategy for the cement industry, particularly if the goal is to achieve deep decarbonisation in alignment with the Paris Agreement.

4. Conclusions

Energy consumption and CO_2 production modelling using Aspen Plus was carried out for six technological options aimed at decarbonising the cement production process. Concerning total energy consumption, the oxyfuel combustion process (Oxy) fuelled by natural gas was found to be the most efficient, requiring approximately 35 % less energy input compared to the reference process, which assumed the use of amine-based post-combustion CO_2 capture in a conventional cement plant powered by natural gas. This highlights the significant potential benefit of oxyfuel combustion, which outweighs the energy requirements of the ASU necessary for the process Oxy.

In the processes using H_2 (i.e., H2-a, H2-b, and H2-c), the total energy reduction compared to the reference process was between 11 % and 33 %. This lower achievement can be attributed to the energy losses in water electrolysis, which became more significant on a per-tonne clinker basis as the level of H_2 substitution increased. Improved electrolysis efficiencies were shown to lead to a significant reduction in total energy in these processes. The process with indirect calcination (in H2-b) required higher H_2 fuel input and eventually consumed more total energy than its counterpart, despite eliminating the need for ASU for O_2 supply.

In terms of CO_2 production, the natural gas-powered oxyfuel-

Table 6
Flue gas composition and CO_2 produced.

Processes	Location	Flue gas (kmol/h)	Flue Gas (kg/h)	Flue Gas (°C)	CO_2 mol fraction	H_2O mol fraction	N_2 mol fraction	CO_2 (kg/t clinker)
NG	Preheater exhaust	64.67	2001.46	130	0.27	0.15	0.57	771.82
Oxy	Preheater exhaust	27.85	963.14	130	0.64	0.36	0.00	781.26
H2-a	Preheater exhaust	28.00	954.61	130	0.62	0.38	0.00	762.13
H2-b	Preheater exhaust	19.60	730.56	130	0.74	0.26	0.00	637.04
H2-b	Calciner combustor exhaust	30.07	741.04	130	0.00	0.35	0.65	0.00
H2-c	Preheater exhaust	29.26	906.73	130	0.49	0.50	0.00	637.04
H2-d	Preheater exhaust	29.59	863.49	130	0.43	0.57	0.00	559.11

combustion (Oxy) process resulted in slightly higher CO_2 generation than the reference plant due to the minor increase in natural gas requirements. The processes utilising H_2 achieved a 17.5 % to 27.6 % reduction in CO_2 generation compared to the reference plant, depending on the level of H_2 substitution, with the highest reduction corresponding to 100 % replacement of natural gas with H_2 in process H2-d. This underscores the potential of H_2, or other low-carbon, in reducing CO_2 generation and emphasizes the importance of integrating energy-focused solutions with efforts targeting raw materials to achieve more comprehensive decarbonisation of cement production. In particular, future research should explore new forms of raw meal for clinker production that reduce the fraction of limestone, a major source of CO_2 generation due to calcination and investigate alternative cementitious materials to reduce the use of conventional clinkers.

CRediT authorship contribution statement

Franco Williams: Conceptualization, Methodology, Investigation, Software, Writing – original draft. **Aidong Yang:** Conceptualization, Supervision, Validation, Writing – review & editing. **Daya Ram Nhuchhen:** Validation, Writing – review & editing.

Declaration of competing interest

The authors declare that they have no known competing financial interests or personal relationships that could have appeared to influence the work reported in this paper.

Data availability

Data will be made available on request.

Appendix A. Supplementary data

Supplementary data to this article can be found online at https://doi.org/10.1016/j.enconman.2023.117931.

References

[1] Churkina G, Organschi A, Reyer CPO, Ruff A, Vinke K, Liu Z, et al. Buildings as a global carbon sink. Nat Sustain 2020;3:269–76. https://doi.org/10.1038/s41893-019-0462-4.

[2] El-Emam RS, Gabriel KS. Synergizing hydrogen and cement industries for Canada's climate plan–case study. Energy Sources Part A 2021;43:3151–65. https://doi.org/10.1080/15567036.2021.1936699.

[3] Nhuchhen DR, Sit SP, Layzell DB. Alternative fuels co-fired with natural gas in the pre-calciner of a cement plant: Energy and material flows. Fuel 2021:295. https://doi.org/10.1016/j.fuel.2021.120544.

[4] Pamenter S, Myers RJ. Decarbonizing the cementitious materials cycle: A whole-systems review of measures to decarbonize the cement supply chain in the UK and European contexts. J Ind Ecol 2021;25:359–76. https://doi.org/10.1111/jiec.13105.

[5] Bouaissi A, Yuan Li L, Mustafa Al Bakri Abdullah M, Ahmad R, Abdul Razak R, Yahya Z. Fly Ash as a Cementitious Material for Concrete. Zero-Energy Buildings - New Approaches and Technologies, IntechOpen; 2020. https://doi.org/10.5772/intechopen.90466.

[6] Velpuri VSB, Jyothishya BCK, Vinod Y. Experimental studies on durability properties of Sustainable and Eco-friendly materials of GGBS and Fly ash in reinforced cement concrete. In: IOP Conf Ser Earth Environ Sci, vol. 796. IOP Publishing Ltd; 2021. https://doi.org/10.1088/1755-1315/796/1/012070.

[7] Teixeira ER, Mateus R, Camões AF, Bragança L, Branco FG. Comparative environmental life-cycle analysis of concretes using biomass and coal fly ashes as partial cement replacement material. J Clean Prod 2016;112:2221–30. https://doi.org/10.1016/j.jclepro.2015.09.124.

[8] Khurana S, Banerjee R, Gaitonde U. Energy balance and cogeneration for a cement plant 2002:486–94.

[9] Nie S, Zhou J, Yang F, Lan M, Li J, Zhang Z, et al. Analysis of theoretical carbon dioxide emissions from cement production: Methodology and application. J Clean Prod 2022:334. https://doi.org/10.1016/j.jclepro.2021.130270.

[10] Chatterjee A, Sui T. Alternative fuels – Effects on clinker process and properties. Cem Concr Res 2019:123. https://doi.org/10.1016/j.cemconres.2019.105777.

[11] Rahman A, Rasul MG, Khan MMK, Sharma SC. Assessment of energy performance and emission control using alternative fuels in cement industry through a process model. Energies (Basel) 2017:10. https://doi.org/10.3390/en10121996.

[12] Sanaye S, Khakpaay N, Chitsaz A, Hassan Yahyanejad M, Zolfaghari M. A comprehensive approach for designing, modeling and optimizing of waste heat recovery cycle and power generation system in a cement plant: A thermo-economic and environmental assessment. Energy Convers Manag 2020:205. https://doi.org/10.1016/j.enconman.2019.112353.

[13] Juangsa FB, Cezeliano AS, Darmanto PS, Aziz M. Thermodynamic analysis of hydrogen utilization as alternative fuel in cement production. S Afr J Chem Eng 2022;42:23–31. https://doi.org/10.1016/j.sajce.2022.07.003.

[14] Benhelal E, Shamsaei E, Rashid MI. Challenges against CO2 abatement strategies in cement industry: A review. J Environ Sci (China) 2021;104:84–101. https://doi.org/10.1016/j.jes.2020.11.020.

[15] Faria DG, Carvalho MMO, Neto MRV, de Paula EC, Cardoso M, Vakkilainen EK. Integrating oxy-fuel combustion and power-to-gas in the cement industry: A process modeling and simulation study. Int J Greenhouse Gas Control 2022:114. https://doi.org/10.1016/j.ijggc.2022.103602.

[16] Ying Z, Lixin C, Qiao L, Guozan C, Xuchu Y. Simulating the Process of Oxy-Fuel Combustion in the Sintering Zone of a Rotary Kiln to Predict Temperature, Burnout, Flame Parameters and the Yield of Nitrogen Oxides. Chem Technol Fuels Oils 2018;54:650–60. https://doi.org/10.1007/s10553-018-0971-2.

[17] Nhuchhen DR, Sit SP, Layzell DB. Decarbonization of cement production in a hydrogen economy. Appl Energy 2022:317. https://doi.org/10.1016/j.apenergy.2022.119180.

[18] Ditaranto M, Bakken J. Study of a full scale oxy-fuel cement rotary kiln. Int J Greenhouse Gas Control 2019;83:166–75. https://doi.org/10.1016/j.ijggc.2019.02.008.

[19] Khadka D. Calcination applying H2 combustion in O2 in a CO2 rich atmosphere. University of South Eastern Norway 2021. https://openarchive.usn.no/usn-xmlui/bitstream/handle/11250/2765115/no.usn%3Awiseflow%3A2636125%3A43485478.pdf?sequence=1&isAllowed=y (accessed July 11, 2023).

[20] Association MP, Ltd C. Options for switching UK cement production sites to near zero CO2 emission fuel: Technical and financial feasibility 2019. https://assets.publishing.service.gov.uk/government/uploads/system/uploads/attachment_data/file/866365/Phase_2_-_MPA_-_Cement_Production_Fuel_Switching.pdf (accessed July 11, 2023).

[21] Hanson. Hydrogen trial | Hanson UK 2022. https://www.hanson.co.uk/en/socialvalue/climate/hydrogen-trial (accessed May 9, 2023).

[22] Ozcan DC, Brandani S, Ahn H. A hybrid carbon capture system of indirect calcination and amine absorption for a cement plant. Energy Procedia, vol. 63, Elsevier Ltd; 2014, p. 6428–39. https://doi.org/10.1016/j.egypro.2014.11.678.

[23] Vikström A. Separate Calcination in Cement Clinker Production A laboratory scale study on how an electrified separate calcination step affects the phase composition of cement clinker. 2021.

[24] Institute of Power Engineering. Basic information on hydrogen 2022. https://www.ien.com.pl/tl_files/pliki/CPE/FAQ_final_EN.pdf (accessed April 26, 2023).

[25] Salzgitter. World's largest high-temperature electrolyzer achieves record efficiency. Sunfire 2022. https://www.sunfire.de/en/news/detail/worlds-largest-high-temperature-electrolyzer-achieves-record-efficiency# (accessed April 26, 2023).

[26] Meeting the Dual Challenge: A Roadmap to At-Scale Deployment of Carbon Capture, Use, and Storage Key Excerpts from National Petroleum Council Report: Chapter 6: CO 2 Transport. 2019.

[27] Nhuchhen DR, Sit SP, Layzell DB. Towards net-zero emission cement and power production using Molten Carbonate Fuel Cells. Appl Energy 2022:306. https://doi.org/10.1016/j.apenergy.2021.118001.

[28] Smith R. Chemical Process Design and Integration 2005;2. https://nitsri.ac.in/Department/Chemical%20Engineering/PEDB1.pdf (accessed July 11, 2023).

[29] Wan B. Energy Density of Methane - The Physics Factbook. The Physics Factbook 2004. https://hypertextbook.com/facts/2004/BillyWan.shtml (accessed January 13, 2023).

[30] Voldsund M, Gardarsdottir SO, De Lena E, Pérez-Calvo JF, Jamali A, Berstad D, et al. Comparison of technologies for CO 2 capture from cement production—Part 1: Technical evaluation. Energies (Basel) 2019:12. https://doi.org/10.3390/en12030559.

[31] Moreira LF, Arrieta FRP. Thermal and economic assessment of organic Rankine cycles for waste heat recovery in cement plants. Renew Sustain Energy Rev 2019:114. https://doi.org/10.1016/j.rser.2019.109315.